Journal Name

COMMUNICATION

New Evidence of a Thermodynamically Stable Nanophase: CdS in 4 M KOH-tert-butanol solution

Jinsheng Zheng [*a], XiaogangXue [a], Dongsong Li[a], and Yibing Zhao[b]

Thermodynamically stable nanophases have been confirmed as an important technical means of nano-synthesis. In this work, CdS nanosheets with thickness of 10 nm were confirmed as a new thermodynamically stable phase under hydrothermal conditions in a 4M KOH-tert-butanol solution at 180 °C. Thermodynamically stable phase of CdS varied with the KOH concentration in the system, but the morphology of the nanosheets was independent of the size of the CdS precursor (3 nm, 9 nm, or bulk). The thermodynamically stable nanosheets were consistent with negative effective interfacial free energy of the CdS (001) face of the wurtzite structure. Further research showed the microprocess of transformation into nanosheets from bulk CdS. The new thermodynamically stable nanostructures open up possibilities for industrial mass production of nanomaterials and green synthesis.

Size, shape, and crystal structure are crucial factors in determining the chemical, optical, and electrical properties of nanoscale materials. Therefore, synthesis of nanoparticles with a uniform size and morphology is of great important but remains one of the most significant challenges in nanotechnology.[1-6] One effective kinetic method is by controlling the rate of nanoparticle nucleation and the growth rates of different crystal faces.[7-10] Difficulty then arises because nanoparticles are normally metastable relative to the equivalent bulk material. Due to the inherent thermodynamic tendency, nanoparticles grow into bulk material spontaneously, which complicates kinetic control of size. The spontaneous growth tendency also makes it difficult to recycle nano-materials in the application process due to their morphology change.

An ideal method to realize monodisperse size distribution of nanomaterials is to create a thermodynamically stable nanophase. In our previous work, we proved for the first time that thermodynamically stable nanophase can be achieved in a ZnS + NaOH +H_2O ternary system.[11] By optimizing the concentration of

NaOH, we were able to obtain various thermodynamically stable nanophases with specific sizes and shapes accordingly.[12] We further developed synthetic routes for ZnS nanostructures, applied them in photocatalyis,[13, 14] and demonstrated their superiority in terms of mass production, renewable recycling and green synthesis.

Although the concept of thermodynamically stable nanosystem has been proven experimentally, the universality of the concept is still under investigation. Is the thermodynamically stable nanophase material a universal phenomenon? What is the micromechanism for the formation of thermodynamically stable nanophase? Does this system extend to other popular materials? In 2010, molecular dynamics simulations predicted the existence of a thermodynamically stable colloidal structure with nanometer-size Ta particles suspended in liquid Cu.[15] As an important II–VI group semiconductor, CdS has been applied in photoluminescence,[16] photocatalysis,[17] solar cell,[18] etc. In this work, we report new evidence of the thermodynamically stable nanophase: CdS in 4M KOH-tert-butanol solution under hydrothermal condition at 180 °C. We define the final state of a system as the thermodynamically stable state, by which the existence of thermodynamically stable nanophase can be confirmed by coarsening experiments. Results from this study suggest that the concept of thermodynamically stable nanostructure may extend to other systems. The finding of more thermodynamically stable nanophase may provide a simple and economical method to realize mass production of nanomaterials and green synthesis.

Figure 1 is a brief illustration of the experimental framework of this study based on X-ray diffraction (XRD) spectra. It was found that CdS eventually transformed into the same nanophase in 4 M KOH-tert-butanol solution, irrespective of the initial samples(3nm, 9nm or bulk). (Figure 1a,1b) The XRD spectra indicated that the structure of the final state was a hexagonal wurtzite phase. In contrast, 3nm CdS nanoparticles grew into bulk CdS under hydrothermal condition at 180 °C when the concentration of KOH-tert-butanol solution was less than 3 M. (Figure 1c, supplementary Figures S2)
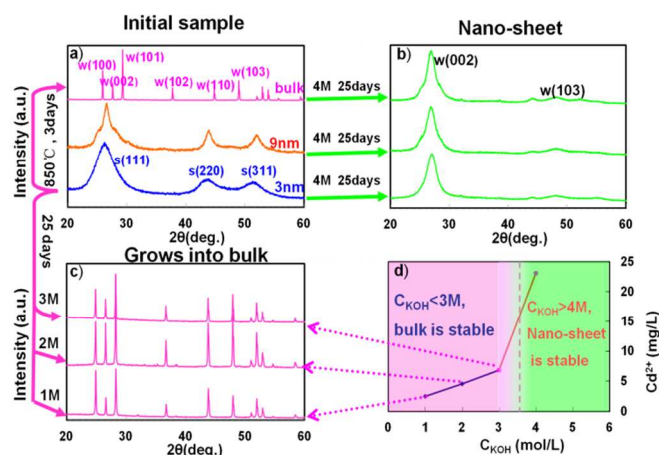
Figure 1. XRD spectra (a, b, c) showing the transformation from the initial CdS sample. a) initial CdS samples, 3 nm CdS (in blue, cubic sphalerite phase), bulk CdS (in purple, hexagonal wurtzite phase), and 9nm CdS (in nacarat, mixture of sphalerite phase and wurtzite phase). b) CdS nanosheets (in green) from various initial CdS samples under hydrothermal condition at 180 °C in 4M KOH-tert-butanol solution. The strong peaks at 26.65° exactly match the (002) peak of hexagonal wurtziteCdS. c) bulk CdS from 3nm CdS treated at 180 °C in KOH-tert-butanol solutions of different concentrations. d) solubility of CdS at 180 °C in KOH-tert-butanol solutions of different concentrations(obtained from ICP analysis).

SEM and TEM images show the nanophase has a sheet like long strip stacking morphology.(Figure 2, Figure 3) From the XRD pattern, a sharp (002) peak can be observed, which is assigned to a strong effect of preferred orientation in the (001) plane contributed by the sheet like morphology. It was difficult to determine the thickness of the nanosheets by TEM or SEM. AFM measurements indicated the thickness of a single sheet to be approximately 8-10 nm (supplementary Figures S3), consistent with Scherrer analysis of the width of the XRD (002) peak.

A CdS nanophase with a sheet like morphology was formed instead of bulk CdS. Our TEM and XRD measurements show that the nanophase materials obtained by the hydrothermal treatment of CdS in 4 M KOH-tert-butanol solution are equivalent whether CdS nanoparticles or bulk CdS were chosen as the starting material. In other words, the nanosheets were the equilibrium form of CdS under the solution conditions. In each case, material with cubic symmetry or hexagonal symmetry was transformed into CdS nanosheets with hexagonal symmetry.

As indicated in Figure 1, the thermodynamically stable phase was found to depend on the concentrations of KOH-tert-butanol solution for CdS under hydrothermal condition at 180 °C. When the concentration was less than 3 M, bulk was stable; when the concentration was up to 4 M, nanosheet was stable. The critical transformation concentration was between 3 M and 4 M. The shape and crystal structure of the nanophase only depended on the molar ratio of compositions in the system and were foreign to CdS precursors. These definitely confirmed the existence of thermodynamically stable nanophase.

The Gibbs free energy analysis can reveal the preferred orientation and morphology of crystals. The Gibbs free energy of nanoparticles is the sum of the Gibbs free energy of bulk materials and an interfacial free energy (IFE): [11, 19, 20]

$$G_{nano} = G_{bulk} + \gamma A \qquad (1)$$

At a certain pressure and temperature, a reaction can only spontaneously proceed from a state with higher free energy(metastable phase) to a state with lower free energy (stable phase). Consequently, in this system, the experimental results showed that CdS nanosheets had lower molar free energy than bulk CdS, i.e., $G_{nano} < G_{bulk}$, $\gamma < 0$.
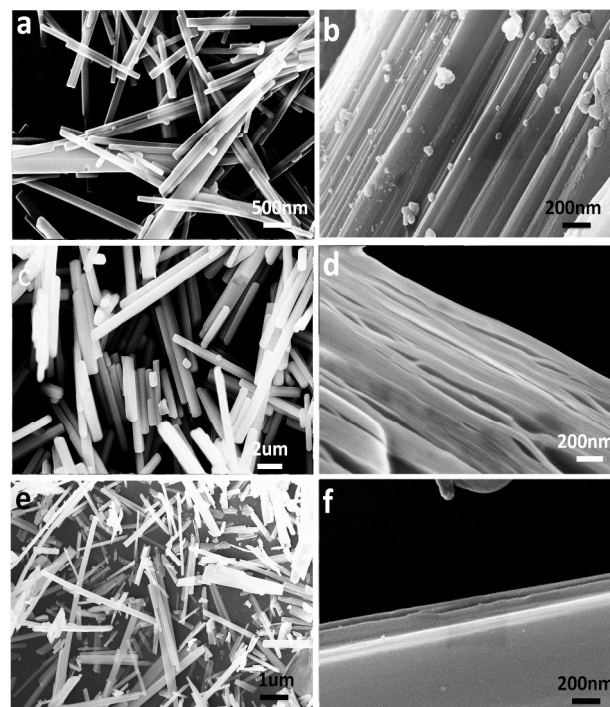

Figure 2. SEM images showing resulting morphologies originated from different initial samples of CdS, all of which coarsened in 4 M KOH-tert-butanol solution at 180 °C for different durations. Large scale (a) and high resolution (b) images of 3 nm CdS coarsened for 7 days. Large scale (c) and high resolution (d) images of 9 nm CdS coarsened for 12 days. Large scale (e) and high resolution (f) images of bulk CdS coarsened for 25 days. The high resolution images give lateral morphology of CdS samples, which clearly show the structure of the sheet-like stacking.
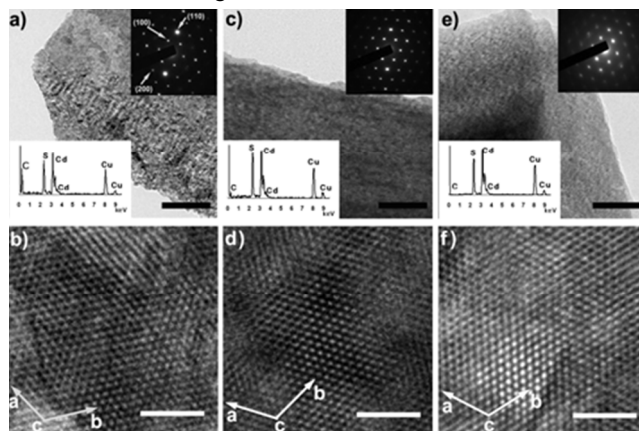

Figure 3. TEM images of CdS nanosheets formed in 4 M KOH-tert-butanol solution at 180 °C. Large scale (a) and high resolution (b) images of sample formed by hydrothermal treatment of 3 nm CdS for 7 days. Large scale (c) and high resolution (d) images of sample obtained by treating 9nm CdS for 12 days. Large scale (e) and high

resolution (f) images of sample obtained by treating bulk CdS for 25 days. Selected area electron diffraction (SAED) and energy-dispersive X-ray (EDX) fluorescence data are given as insets a=4.10Å，c=6.65 Å，fit well with JCPDS card 80–0006. Crystallographic axis directions are indicated on high-resolution images b, d, and f. It was verified by EDX fluorescence measurements that the new nanophase was composed of only Cd and S, with negligible O (inset). The SAED pattern can be indexed as the [001] zone axis of hexagonal wurtzite-type CdS crystal. TEM scal bar: 100 nm in (a) (b)(c), and 2 nm in (d) (e) (f).

If the thermodynamically stable nanophase begins to form, the interfacial energy γ must be effectively negative. In our previous studies, we put forward a theoretical description involving a negative effective interfacial free energy (IFE) to explain thermodynamically stable nanophase .

$$\gamma \cong \gamma_{bulk} - (\mu - \mu_{bulk})\Gamma_{max} \qquad (2)$$

where μ_{bulk} is defined as the value for which $\gamma = \gamma_{bulk}$, and Γ_{max} is the saturated surface adsorbate density.

$$\mu_{CdS,ads} = \mu_{CdS,solution} = \mu_0 + RTln(a_{Cd^{2+}}) \quad (3)^{[21]}$$

For CdS system,

$$\gamma \cong \gamma_{bulk} - (\mu_{CdS,ads} - \mu_{bulk})\Gamma_{max} \qquad (4)$$

Obviously, $\mu_{CdS,solution}$ is relative to the concentrations of Cd^{2+}, which prompts the measurement of the solubility of 3nm CdS in different concentrations of KOH-tert-butanol solution at 180 °C. Results showed that the solubility of CdS increased with the concentration of KOH. When the concentration of KOH was accorded with a negative IFE condition, the concentrations of Cd^{2+} increased abruptly. (Figure 1d) This indicated that the IFE was even lower to the negative region with increasing concentrations of KOH.[22]

The anisotropy of crystal structure leads to different adsorption enthalpies for different termination faces of a material. In our system, the CdS (001) face was determined to be the dominant surface in the nanosheets. Due to CdS being a polar crystal, the polarity of hexagonal (001) plane should be the strongest, which made KOH adsorption easy. The IFE of (001) plane was most affected with the concentration of KOH, and we obtained nanosheets in a single crystallographic dimension [001], possibly because the (001) plane was stabilized in the nanoscale range by OH^-, while the growth of ab plane is not restricted. It can be concluded that the IFE of the CdS (001) face was effectively negative under the condition, whereas the IFE of all other faces remained positive.

In our previous work, we studied ZnS nanosheets in aqueous NaOH solution. Various branched morphologies were obtained by varying NaOH concentrations.[12] However, complex morphologies for the CdS nanosheet in KOH-tert-butanol solution were not obtained since the CdS nanosheets always formed nanosheet stackings. Other than ZnS, thermodynamically stable phase of bulk CdS was a hexagonal wurtzite phase and ZnS a cubic sphalerite phase.[23] Because the polarity of hexagonal wurtzite phase (especially (001) plane) was stronger than cubic sphalerite phase[24], hexagonal wurtzite phase may be more stable under a strong polar interfacial effect. Thus in the ZnS system above, the energy of hexagonal phase decreased to a level close to that of cubic phase. The nucleation probability of hexagonal phase and cubic phase were competing with each other which resulted in various branched morphology. In the CdS system, the hexagonal phase was usually more stable under interfacial effect and the nucleation probability of cubic phase was negligible hence the formation of hexagonal nanosheet stackings occurred. The CdS nanosheet with strong polarity (001) face may possibly self-assemble into nanosheet stackings via thermal perturbation. The possible mechanism of the formation of the nanosheet stackings is shown in supplementary Figure S4.
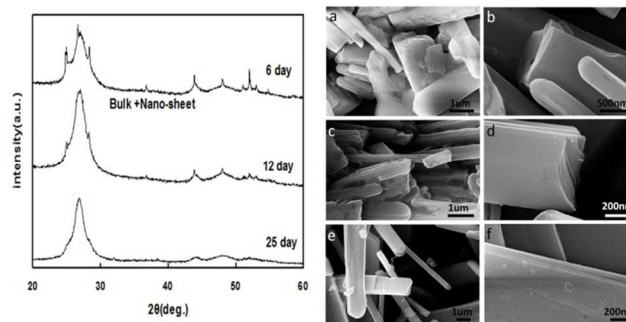

Figure 4. XRD spectra and relevant SEM images of the bulk CdS coarsened in 4M KOH-tert-butanol solution at 180 °C for different durations. The XRD data indicate that when the time for sample treatment was insufficient ,the sample was a mixture of bulk CdS and nanosheet CdS. SEM images showing the the bulk CdS coarsened in 4M KOH-tert-butanol solution at 180 °C for different durations. Large scale (a) and high resolution (b) images for 6 days. Large scale (c) and high resolution (d) images for 12 days.Large scale (e) and high resolution (f) images for 25 days.

To study the formation micromechanism, especially the transition from bulk material to thermodynamically stable nanophase, we examined the different stages of the equilibrium state of CdS nanosheets from bulk samples. (Figure 4) It was found that longer time was needed for the bulk CdS to achieve the desired equilibrium state in KOH-tert-butanol solution. XRD data indicated that bulk CdS was converted to a nanosheet structure gradually. The 6-day sample was mostly nanosheet phase with a small portion of bulk phase. When the hydrothermal time increased to 12 days, the sample basically turned into nanosheet, but there was still residual bulk phase. After 25 days, it was confirmed that the sample completely turned into nanosheet structure. This gradual evolution indicated that the formation of nanosheet was accompanied with the consumption of bulk sample. Further SEM characterization showed the relevant process of transformation into nanosheets from bulk. The interface of the initial bulk sample surface was eroded by solution. As time progressed, nanosheets were converted in situ from bulk and the stacking morphology became increasingly evident.

In our previous work, we confirmed the existence of thermodynamically stable ZnS nanophase under hydrothermal condition in a highly concentrated aqueous NaOH solution at 230 °C. Considering ZnS and CdS are both polar crystal, we used similar conditions for CdS. However, CdS nanoparticles grew quickly into bulk under these conditions. Fortunately, we observed similar thermodynamically stable ZnS or CdSe nanophase under the same hydrothermal condition in 4M KOH-tert-butanol solution at 180 °C. (See the supporting information Figure S5&S6) To explain different results between ZnS and CdS, the increased basicity of the KOH-tert-butanol solution as compared to the aqueous NaOH solution was taken into consideration. It was surmised that the interfacial effect on the surface of a polar crystal increased with solution basicity. As a result, KOH-tert-butanol solution exerted more interfacial effect on CdS surface than aqueous NaOH solution. Besides, ZnS may react to NaOH in aqueous NaOH solution, the solubility of ZnS increased as Na_2ZnO_2 was formed. Conversely, it was difficult for CdS to react with NaOH, and the polarity of CdS was weaker than that of ZnS. Consequently, thermodynamically stable CdS nanophase was only obtained in KOH-tert-butanol solution.

Conclusions

In conclusion, a new thermodynamically stable nanophase, i.e. CdS nanosheets was obtained in 4M KOH-tert-butanol solution under hydrothermal conditions at 180 °C, and the micromechanism was investigated. Further study showed that the thermodynamically stable nanophase could extend to more materials, other thermodynamically stable nanosystems should be developed and verified. This work deepens the understanding of the thermodynamically stable nanophase and opens up possibilities of mass production of nanomaterials.

ACKNOWLEDGMENT

Notes and references

[a] State Key Lab of Structural Chemistry, Fujian Institute of Research on the Structure of Matter, Chinese Academy of Sciences, Fuzhou, Fujian, 350002, China. E-mail: jszheng@fjirsm.ac.cn

[b] College of Chemistry and Chemical Engineering, Xiamen University, Xiamen, Fujian, 361005, China.

1 S. H. Sun, C. B. Murray, D. Weller, L. Folks and A. Moser, *Science*, 2000, **287**, 1989-1992.

2 Z. F. Ding, B. M. Quinn, S. K. Haram, L. E. Pell, B. A. Korgel and A. J. Bard, *Science*, 2002, **296**, 1293-1297.

3 E. V. Shevchenko, D. V. Talapin, C. B. Murray and S. O'Brien, *J. Am. Chem. Soc.*, 2006, **128**, 3620-3637.

4 A. N. Cao, Z. Liu, S. S. Chu, M. H. Wu, Z. M. Ye, Z. W. Cai, Y. L. Chang, S. F. Wang, Q. H. Gong and Y. F. Liu, *Adv. Mater.*, 2010, **22**, 103-+.

5 R. Costi, A. E. Saunders and U. Banin, *Angew. Chem. Int. Ed.*, 2010, **49**, 4878-4897.

6 J. M. R. Tan, Y. H. Lee, S. Pedireddy, T. Baikie, X. Y. Ling and L. H. Wong, *J. Am. Chem. Soc.*, 2014, **136**, 6684-6692.

7 M. P. Pileni, *Nat. Mater.*, 2003, **2**, 145-150.

8 Y. W. Jun, J. S. Choi and J. Cheon, *Angew. Chem. Int. Ed.*, 2006, **45**, 3414-3439.

9 K. M. O. Jensen, M. Christensen, P. Juhas, C. Tyrsted, E. D. Bojesen, N. Lock, S. J. L. Billinge and B. B. Iversen, *J. Am. Chem. Soc.*, 2012, **134**, 6785-6792.

10 L. Zhang, Y. Wang, L. M. Tong and Y. A. Xia, *Nano Lett.*, 2014, **14**, 4189-4194.

11 Z. Lin, B. Gilbert, Q. L. Liu, G. Q. Ren and F. Huang, *J. Am. Chem. Soc.*, 2006, **128**, 6126-6131.

12 G. Q. Ren, Z. Lin, B. Gilbert, J. Zhang, F. Huang and J. K. Liang, *Chem. Mater.*, 2008, **20**, 2438-2443.

13 D. S. Li, Z. Lin, G. Q. Ren, J. Zhang, J. S. Zheng and F. Huang, *Cryst. Growth Des.*, 2008, **8**, 2324-2328.

14 D. G. Chen, F. Huang, G. Q. Ren, D. S. Li, M. Zheng, Y. J. Wang and Z. Lin, *Nanoscale*, 2010, **2**, 2062-2064.

15 T. Frolov and Y. Mishin, *Phys. Rev. Lett.*, 2010, **104**.

16 O. Chen, J. Zhao, V. P. Chauhan, J. Cui, C. Wong, D. K. Harris, H. Wei, H. S. Han, D. Fukumura, R. K. Jain and M. G. Bawendi, *Nat. Mater.*, 2013, **12**, 445-451.

17 L. Amirav and A. P. Alivisatos, *J. Phys. Chem. Lett.*, 2010, **1**, 1051-1054.

18 Z. X. Pan, H. Zhang, K. Cheng, Y. M. Hou, J. L. Hua and X. H. Zhong, *ACS nano*, 2012, **6**, 3982-3991.

19 Z. Lodziana, N. Y. Topsoe and J. K. Norskov, *Nat. Mater.*, 2004, **3**, 289-293.

20 A. Mathur, P. Sharma and R. C. Cammarata, *Nat. Mater.*, 2005, **4**, 186-186.

21 Here $\mu_{CdS,ads}$ stands for the chemical potential of interfacial CdS; $\mu_{CdS,solution}$ stands for the chemical potential of CdS in solution; μ_0 stands for the chemical potential of CdS under standard state; $a_{Cd^{2+}}$ stands for the activity of Cd^{2+}.

22 According to Formula 3&4, $\gamma \cong \gamma_{bulk} - \left(\mu_{CdS,ads} - \mu_{bulk}\right)\Gamma_{max} = \gamma_{bulk} - \left(\mu_0 + RT\ln(a_{Cd^{2+}}) - \mu_{bulk}\right)\Gamma_{max}$, when $a_{Cd^{2+}}$ increase, γ will decrease even lower to the negative region.

23 Kryukov, A.I.; YaKuchmii S.; Pokhodenko, V.D. Theor. Exp. Chem. 2000, **36**, p. 73.

24 Handbook, Physico-Chemical Properties of Semiconductor Compounds, Nauka, Moscow (1979).

4792x4588mm (3 x 3 DPI)